A Novel Model for Bicycle Drivetrain Efficiency

Teal Dowd[1], Patrick Cavanaugh[1] and Jan-Anders Mansson[1*]

[1*]Purdue University, Ray Ewry Sports Engineering Center (RESEC), 1105 Endeavour Drive Suite 200, West Lafayette, 47906, IN, USA.

*Corresponding author(s). E-mail(s): jmansson@purdue.edu;

Abstract

This study introduces a new model for bicycle drivetrain efficiency, termed the "DC" (Dowd-Cavanaugh) model. This model is a comprehensive approach for characterizing cycling drivetrain efficiency across varying conditions—a critical factor in optimizing the performance of bicycles in competitive, recreational, and transportation contexts. A specialized testing rig was developed to measure drivetrain efficiency under different simulated riding conditions, with a particular focus on the performance of chains using various lubricants over varied torque and RPM conditions. Analysis revealed a linear relationship ($\boldsymbol{R^2 > 0.999}$) between efficiency and the DC metric, defined as $\boldsymbol{DC_{metric} = \frac{RPM^{0.3}}{Torque}}$, providing a comprehensive framework for predicting drivetrain efficiency. Through regression analysis, the slope and intercept of this linear relationship were employed as all-encompassing parameters characterizing drivetrain performance, facilitating targeted lubricant selection based on specific cycling scenarios. The DC model establishes a robust framework for advancing both practical applications and scientific understanding of cycling drivetrain efficiency. The broad applicability of the DC model in analyzing efficiency across different situations offers substantial opportunities for optimizing drivetrain performance, especially in aligning mechanical and physiological efficiencies for prolonged, lower power outputs.

Keywords: cycling, lubrication, efficiency, modeling

1 Introduction

In competitive cycling, the pursuit of performance optimization is characterized by an accumulation of marginal gains, where incremental improvements across various aspects contribute to enhanced overall efficiency. While air resistance accounts for the majority of energy loss, particularly at high speeds, other factors such as rolling resistance, rider and bike mass, and drivetrain resistance also play significant roles. The drivetrain refers to the system responsible for transferring power from the rider to the wheels, consisting of the pedals, chain, chainrings, cassette, derailleur, and crankset. Drivetrain resistance constitutes a consistent component of overall cycling resistance over all cycling conditions, while air resistance is highly dependent on speed and can account for 40-70% of the total resistance [1, 2].

Significant works have been done on the aerodynamic losses of cycling [2], but less work has focused on characterization of the drivetrain efficiency. A variety of labs have created full-scale or component-level testing rigs to measure the efficiency of cycling drivetrains [3–13]. A review article by Aubert *et al.* [14] summarized many of these measurement systems. These testing rigs typically included a motor driving a chain against a resistance mechanism, with power sensors to determine the transmission efficiency.

Other methods of measuring drivetrain efficiency have been developed, such as the pendulum-type mechanism [5, 15]. This method is very accurate at measuring roller chain efficiency, but abstracts many parts of a realistic cycling drivetrain such as the derailleur and non-symmetric loads between the top (load carrying) and bottom (return) chain paths. As Aubert *et al.* [14] concluded, these different methods of measuring drivetrain efficiency have their respective advantages and disadvantages. The more representative the testing device, the less precise it tends to be. Conversely, while isolating variables can lead to higher precision, it comes at the cost of reduced applicability to real-world conditions.

Previous publications [4–6] found a linear relationship between the drivetrain and the reciprocal of the chain tension. This relationship is expressed in **Eq. 1**, where chain tension is replaced by drivetrain torque, as the two quantities are directly proportional through the chainring diameter. Other work has suggested separately that increasing rotational speed decreases efficiency [4, 7–9]. The present research proposes a new model for drivetrain efficiency, termed the "DC Model" named after those who made the discovery. This model combines rotational speed and torque into a new metric used as the independent variable for an equation predicting drivetrain efficiency. The new model improves the ability to predict efficiency over a wide range of torque and rotational speeds.

$$\eta_{drivetrain} \propto \left(\frac{1}{torque}\right) \tag{1}$$

2 Methods

The DC model for bicycle drivetrain efficiency introduced in this work necessitated the collection and analysis of testing data for model development. The following sections provide insight into the data collection process that facilitated the observations leading to the formulation of the new model.

2.1 Testing Rig

The bicycle drivetrain efficiency testing rig utilized in this study was adapted from prior work focused on smart trainer testing by Dowd *et al.* [16, 17], and expanded to enable comprehensive evaluation of cycling drivetrains. **Fig. 1** shows the testing rig with all major components, capable of testing drivetrains under a variety of conditions with a particular focus on those most commonly encountered during normal cycling.

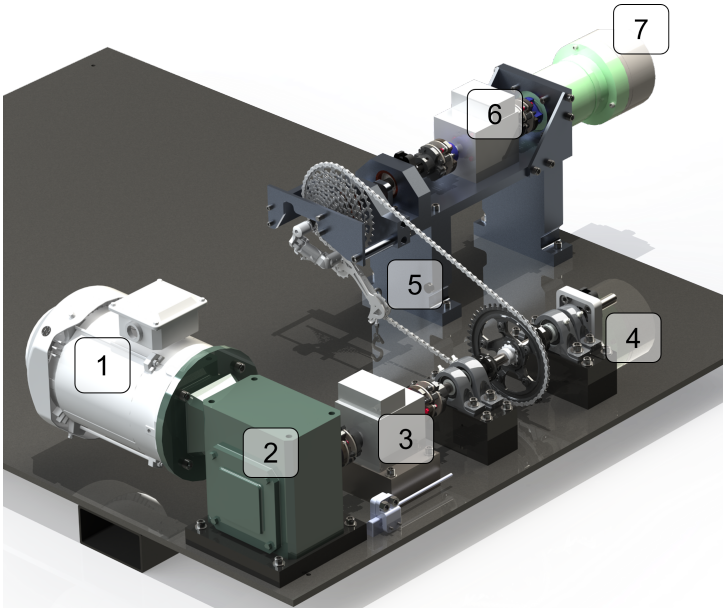

Fig. 1: Testing rig render with components: 1) Motor, 2) 5:1 gearbox, 3) input power torque transducer, 4) rotary encoder, 5) cycling drivetrain, 6) output power torque transducer, 7) Electromagnetic brake

2.2 Experimental Setup

All data collected was tested using a Shimano Ultegra 11-speed chain (CN-HG701-11) with 112 links. Two example lubricants were used, as presented in **Table 1**. The lubricants consisted of a wax-based immersion type and

a dry-type drip lubricant. The developed DC model aids in illustrating the differences between these two lubricants.

Lubricant Designation	Type
Lubricant A	Wax immersion lubricant
Lubricant B	Drip lubricant

Table 1: Lubricants used for drivetrain efficiency comparison using the DC model

The testing procedure commenced with a chain that underwent a comprehensive cleaning process. This multi-stage cleaning method was based on established protocols [18]. Initially, the chain was immersed in a container filled with mineral spirits and manually agitated. Subsequently, the container was placed in a water ultrasonic bath. Following this, the chain was extracted, wiped down with a towel, and transferred to a new container. This sequence was repeated three additional times to ensure thorough cleaning. A final round was conducted using denatured alcohol to remove the mineral spirits. To eliminate any residual moisture, the chain was then placed in an oven at $80°C$ for 20 minutes.

The application of wax-based lubricants was performed following a procedure adapted from established methodology [19]. A small ceramic dish containing the wax lubricant was placed inside an industrial oven and heated to 80°C until the wax was fully melted. The chain, which had been predried and preheated to 80°C, was then fully submerged in the molten wax and agitated to ensure comprehensive coverage. After removal from the wax, the chain was allowed to cool to ambient temperature before being installed on the testing rig for experimentation.

The application of dry-based lubricants was conducted in accordance with the manufacturers' instructions. The general protocol involved depositing multiple thick drops of lubricant onto each chain link, followed by the removal of excess lubricant using a cloth. The treated chain was then allowed to rest for a specified period, typically several hours, prior to testing.

2.3 Experimental Procedure

The primary testing procedure employed in this study was consistent with the methodology outlined by Dowd *et al.* [16]. The testing conditions, denoted by the blue ⋆, are presented in **Fig. 2**. These conditions covered a power range of 200 to 800 watts, with input shaft rotational speeds varying from 76 rpm to 350 rpm. Testing was conducted using a 42-tooth cassette sprocket, yielding a 1:1 gear ratio.

A secondary testing procedure was developed to evaluate drivetrain efficiency under conditions that more closely simulate realistic cycling scenarios, and is presented in **Fig. 3, blue** ⋆. The cycling cadence (rotational

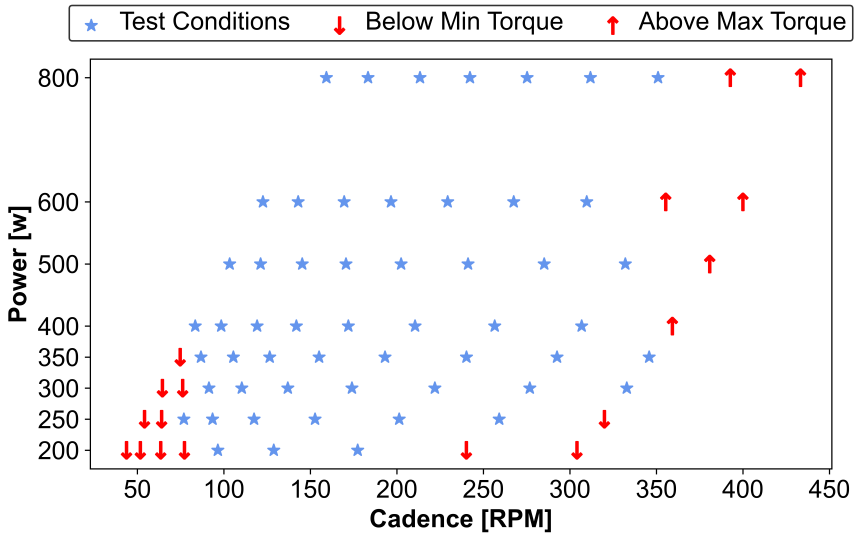

Fig. 2: Experimental conditions for wide-range chain characterization. Blue stars (⋆) represent tested points. Red symbols indicate excluded conditions: upward arrows (↑) for drive torque exceeding torque sensor maximum, downward arrows (↓) for brake torque below minimum

speed) was varied between 60 and 120 RPM, while the power level was adjusted between 200 and 500 watts. These tests were conducted using a 17-tooth cassette sprocket, which provided a 42:17 (2.47:1) gear ratio. This ratio was selected to facilitate testing across a wide range of conditions while maintaining relevance to real-world cycling applications.

For both the primary and secondary testing procedures, certain conditions at low speeds and high power levels were omitted due to torque measurements exceeding the safe operational limits of the torque transducer, shown as red ↑ in **Figs. 2** & **3**. Additional conditions with high cadence and low power were excluded as the required resistance torque fell below the minimum resistance threshold of the magnetic brake, shown as red ↓ in **Figs. 2** & **3**. Each test point was run for a duration of 60 seconds, followed by a cooling period to allow the brake to reduce temperature before proceeding to the next test point.

2.4 Drivetrain Efficiency Model

Prior to the development of the DC model, drivetrain efficiency data were plotted as efficiency versus the reciprocal of torque, as shown in **Section 3**. This approach was adopted based on previous literature, which demonstrated its effectiveness in predicting drivetrain efficiency across various testing conditions [4–6]. A regression analysis was performed on these data points, and the resulting slope and intercept were utilized to comprehensively characterize

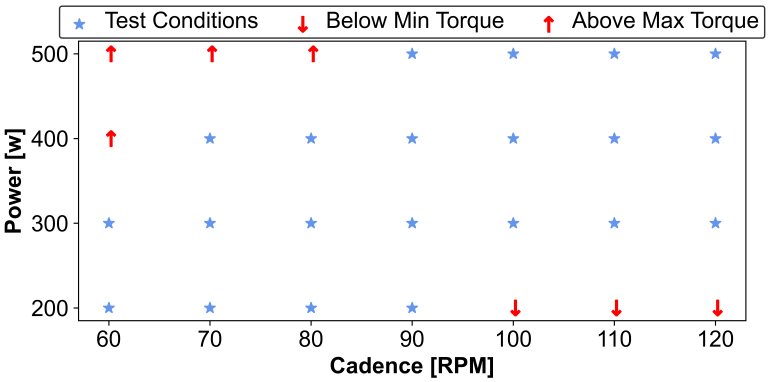

Fig. 3: Realistic cycling experimental conditions for chain characterization. Blue stars (⋆) represent tested points. Red symbols indicate excluded conditions: upward arrows (↑) for drive torque exceeding torque sensor maximum, downward arrows (↓) for brake torque below minimum

the overall drivetrain efficiency. Using only the slope and intercept, the efficiency for any given test condition could be calculated using **Eq. 2**.

$$\eta_{drivetrain} = slope \cdot \frac{1}{Torque} + intercept \tag{2}$$

Continued characterization of drivetrain efficiency using the primary testing procedure revealed the presence of an additional variable affecting efficiency beyond torque alone. A closer examination of speed effects on efficiency uncovered a significant relationship: efficiency decreased as rotational speed (rpm) increased. This secondary effect within the reciprocal torque relationship is depicted in **Fig. 4**.

Analysis of this secondary relationship identified a power function as the most accurate representation of the observed pattern. Through curve fitting and exponent optimization, a new relationship was established, expressed by **Eq. 3**. This novel metric was subsequently designated the "Dowd-Cavanaugh Metric," in recognition of the principal researchers who first identified this phenomenon.

$$DC_{metric} = \frac{RPM^{0.3}}{Torque} \tag{3}$$

The utilization of this new DC model significantly enhances the predictive capability by incorporating rotational speed (rpm) into the efficiency equation by better capturing the efficiency profile than torque alone as a dependent variable. The enhanced equation for calculating efficiency under any test condition is provided in **Eq. 4**.

$$\eta_{drivetrain,DC} = slope_{DC} \cdot \left(\frac{RPM^{0.3}}{Torque}\right) + intercept_{DC} \tag{4}$$

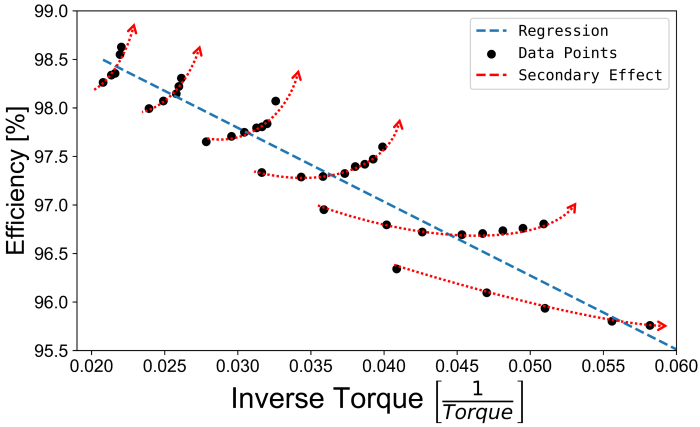

Fig. 4: Secondary effect within the reciprocal torque - efficiency relationship, where the arrows indicate increasing rotational speed [RPM]

2.5 Data Presentation

The uncertainty in both the slope and intercept values for all plotted drivetrain efficiency data was determined through standard margin of error calculations, which were derived from ordinary least squares (OLS) regression. The critical t-value (t_{crit}) was computed using **Eq. 6**, which uses the Probability Point Function (PPF) with a significance level $\alpha = 0.05$ and degrees of freedom, ν, equal to the number of residuals from the OLS regression. The standard error (SE) was calculated from the OLS regression result using **Eq. 5**. Subsequently, the margin of error was determined using **Eq. 7**.

$$SE = \frac{\sqrt{\frac{\sum(y_i - \hat{y}_i)^2}{n-2}}}{\sqrt{\sum(x_i - \bar{x})^2}} \tag{5}$$

$$t_{crit,\alpha/2} = t_{ppf}(1 - \alpha/2, \nu) \tag{6}$$

$$MOE = t_{crit,\alpha/2} \cdot SE \tag{7}$$

Where y_i represents the observed values, $\hat{y}_i$ the predicted values, n the number of observations, x_i the independent variable values, and $\bar{x}$ the mean of the independent variable.

To assess the goodness of fit for the linear regression models, the coefficient of determination (R^2) and the root mean square error (RMSE) were calculated. These metrics are reported alongside the plotted regression line slope and intercept values to provide a quantitative measure of the model's fit to the data.

Representative cycling condition were selected for illustrating the drivetrain efficiency and are shown in **Table 2**. The riding gradient and speed

estimates were derived using the ANT+ formula, which is commonly employed in virtual cycling applications [20].

Condition	**Power [W]**	**Gear Ratio**	**Cadence [RPM]**	**Gradient [%]**	**Speed [KpH]**
Uphill	300	42:17	60	5.3	19.6
Flat			90	2.0	29.3
Downhill			120	-0.7	39.1

Table 2: Simulated Cycling Conditions

3 Results

Fig. 5 shows the results of applying the DC model to drivetrain characterization results. **Fig. 5a** shows the efficiency regression using the inverse torque metric, and **Fig. 5b** using the DC metric.

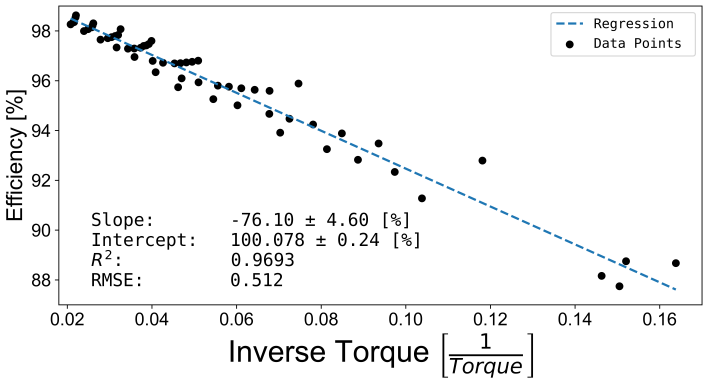

(a)

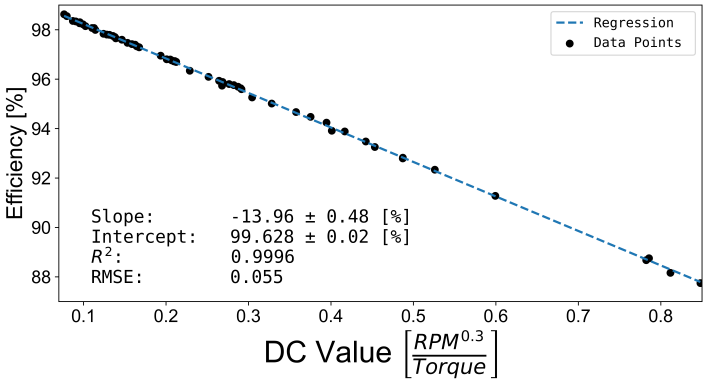

(b)

Fig. 5: Regression fit without the DC model (a) and using the DC model (b)

Fig. 6 employs the DC model to illustrate the difference between two drivetrains using lubricants A and B across the tested realistic conditions, as described in **Fig. 3**. The plotted lines are the DC model regression of the tested points. The left side of the figure, characterized by low DC values, corresponds to higher torque and lower speed conditions, while the right side, exhibiting higher DC values, represents lower torque and higher speed conditions.

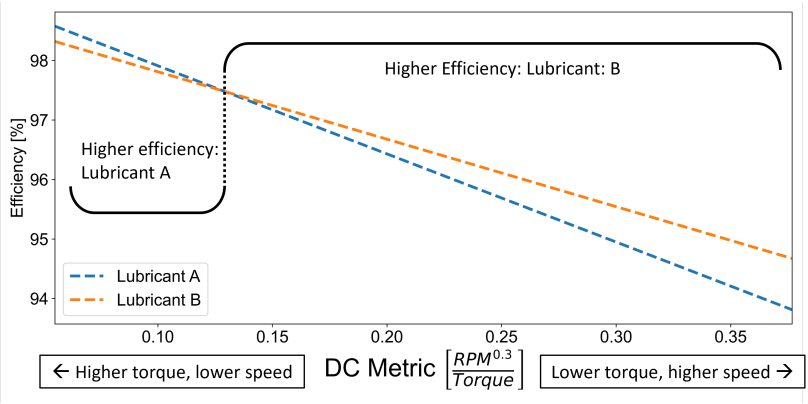

Fig. 6: Drivetrain efficiency characterized over a range of DC values

Fig. 7 compares the maximum achieved efficiency of lubricant A and lubricant B under each of the three simulated cycling condition shown in **Table 2** using the realistic cycling test conditions, as shown in **Fig. 3**. The efficiency is also converted into "Watts Lost" as another way of displaying the efficiency, a common reporting method used by other groups [21, 22].

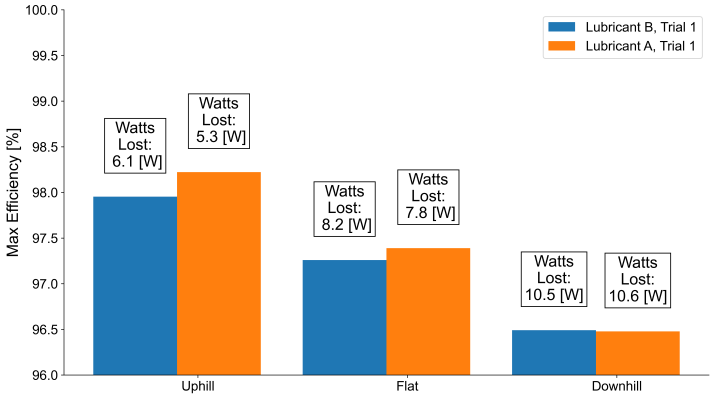

Fig. 7: Bar plot of multiple simulated conditions and their max efficiency using lubricant A and lubricant B

4 Discussion

The DC model enhances the understanding of the components influencing cycling drivetrain efficiency. An example characterization test, illustrated in **Fig. 5**, demonstrates the improved performance of the DC model. The coefficient of determination, R^2, increased from 0.9693 when using inverse torque metric (**Fig. 5a**) to 0.9996 with the DC metric (**Fig. 5b**). This substantial improvement in R^2 was accompanied by a corresponding decrease in Root Mean Square Error (RMSE) from 0.512 to 0.055. This enhancement in statistical measures extends beyond this specific example to all characterization tests conducted.

The DC model slope and intercept values are utilized in calculating specific drivetrain efficiency under any condition using **Eq. 4**. The DC model slope and intercept serve as comprehensive measures of overall drivetrain efficiency. The DC model enables the reporting of efficiency not only for a specific condition, but across a range of scenarios, as the slope and intercept values encapsulate the overall efficiency behavior. The DC model intercept indicates the efficiency at a theoretical infinite torque, zero speed condition, suggesting the presence of certain speed- and torque-independent parasitic losses. The DC model slope represents the rate at which efficiency deteriorates as speed increases and torque decreases.

The characteristic plot of efficiency presented in **Fig. 6** demonstrates how the newly introduced DC model can be employed to visualize drivetrain efficiency under various conditions. Lower DC values, corresponding to higher torque and lower speed conditions, appear on the left side of the plot. Higher DC values, corresponding to higher speed and lower torque conditions, are positioned on the right side. A comparison of drivetrain efficiency using two example lubricants revealed a significant crossover point: lubricant A exhibited superior performance at lower DC values, whereas lubricant B demonstrated superior efficiency at higher DC values. The ability to identify the optimal performance regime for different lubricants based on the DC model proves invaluable for personalizing lubricant selection, particularly when considering specific cycling disciplines and their unique demands. For instance, race mechanics can leverage this information to select the most suitable lubricant for a given event, thereby ensuring peak drivetrain and rider performance.

Fig. 7 illustrates the comparative impact of various cycling conditions on drivetrain efficiency using lubricants A and B. This plot demonstrates that high-torque, low-speed conditions yield higher efficiency than high-speed, low-torque scenarios. Additionally, it shows that some differences in lubricant performance can be compensated for by reducing cadence, thus decreasing the DC value and increasing efficiency.

The potential ramifications of the DC model are not only limited to mechanical performance, but extend to the total mechanical-physiological system of the bike and rider. Determination of an optimal cycling cadence requires a delicate balance between drivetrain mechanics, environmental factors, and human physiology. A comprehensive review conducted by

MacDougall *et al.* [23] highlighted research indicating that metabolic efficiency increases with decreasing cadence at lower power outputs, primarily due to the dominance of slow-twitch muscle activity. At higher power outputs, the metabolic disadvantages of increased cadence are mitigated by the critical role of fast-twitch muscles in producing high power. Similar conclusions were drawn in previous reviews by Abbiss *et al.* [24], Hansen *et al.*, and Ettema *et al.* [25]. The convergence of these findings, particularly the observation that high-torque, low-speed conditions are more advantageous for drivetrain efficiency, and that lower cadences may be physiologically favorable at lower power outputs, indicates a possible interaction between mechanical and biological factors in cycling. This hypothesis warrants further exploration into the possibility of optimizing the total efficiency of the rider-drivetrain system through cadence reduction, especially for long-distance, lower-power scenarios. Such research could lead to refined strategies aimed at enhancing overall cycling efficiency, with implications for both competitive cycling and the broader scope of human-powered transportation.

By leveraging the DC model, the efficiency under various conditions can be plotted. Setting the RPM and torque values of the requested condition, calculating the DC value, and combining that with the known DC model regression slope and intercept for the drivetrain configuration from testing (lubricant, derailleur, and gear ratio combination) allows for the generation of a plot for a variety of conditions to determine efficiency.

5 Conclusion

This study has introduced the "DC" (Dowd-Cavanaugh) model, a novel and comprehensive approach for quantitatively analyzing cycling drivetrain efficiency across varied conditions. By utilizing the slope and intercept of the DC metric regression, the DC model provides a robust method to calculate and predict drivetrain performance beyond the limitations of traditional single-condition efficiency metrics. This capability is particularly advantageous, as it enables the evaluation of drivetrain efficiency across a spectrum of operating conditions, offering a more holistic efficiency profile. The slope and intercept derived from the DC model thus serve as powerful, all-encompassing metrics, which can assist mechanics and engineers in selecting the most suitable lubricant based on anticipated cycling scenarios, ultimately contributing to optimized drivetrain performance. Future work will attempt to identify how the DC model slope and intercept are related physical characteristics of the drivetrain configuration and the lubricant system.

Acknowledgements

Thank you to the Ray Ewry Sports Engineering Center (RESEC) at Purdue University for financial support on this project. Additional thanks to Josh Poertner for supplying chains, lubricants, and expertise.

Conflict of Interest

The authors declare that they have no conflict of interest.

Data availability

Data sets generated during the current study are available from the corresponding author on reasonable request.

References

[1] C. White. Types of Resistance When Cycling. URL https://ridefar.info/bike/cycling-speed/resistance-types/

[2] F. Malizia, B. Blocken (2020), Bicycle aerodynamics: History, state-of-the-art and future perspectives. Journal of Wind Engineering and Industrial Aerodynamics **200**(November 2019), 104,134. https://doi.org/10.1016/j.jweia.2020.104134. URL https://doi.org/10.1016/j.jweia.2020.104134https://linkinghub.elsevier.com/retrieve/pii/S0167610520300441

[3] A. Egorov, K. Kozlov, V. Belogusev (2015), A method for evaluation of the chain drive efficiency. Istrazivanja i projektovanja za privredu **13**(4), 277–282. https://doi.org/10.5937/jaes13-9170. URL http://scindeks.ceon.rs/Article.aspx?artid=1451-41171504277E

[4] J.B. Spicer, C.J.K. Richardson, M.J. Ehrlich, J.R. Bernstein, M. Fukuda, M. Terada (2001), Effects of Frictional Loss on Bicycle Chain Drive Efficiency. Journal of Mechanical Design **123**(4), 598–605. https://doi.org/10.1115/1.1412848. URL https://asmedigitalcollection.asme.org/mechanicaldesign/article/123/4/598/445688/Effects-of-Frictional-Loss-on-Bicycle-Chain-Drive

[5] M.D. Kidd, N. Loch, R. Reuben, Bicycle chain efficiency. Ph.D. thesis, Heriot-Watt University Edinburgh (2000). https://doi.org/10.1201/9781003078098-37. URL https://www.taylorfrancis.com/books/9781000100075/chapters/10.1201/9781003078098-37

[6] J.B. Spicer (2013), Effects of the nonlinear elastic behavior of bicycle chain on transmission efficiency. Journal of Applied Mechanics, Transactions ASME **80**(2). https://doi.org/10.1115/1.4007431. URL https://asmedigitalcollection.asme.org/appliedmechanics/article/doi/10.1115/1.4007431/370715/Effects-of-the-Nonlinear-Elastic-Behavior-of

[7] C.J. Lodge (2000), Experimental Measurements of Roller Chain Transmission Efficiency. Proc. Int. Conf. Gearing, Transmissions, and Mechanical Systems pp. 603–612

[8] S.P. Zhang, T.O. Tak (2020), Efficiency Estimation of Roller Chain Power Transmission System. Applied Sciences **10**(21), 7729. https://doi.org/10.3390/app10217729. URL https://www.mdpi.com/2076-3417/10/21/7729

[9] C.J. Lodge, S.C. Burgess (2002), A model of the tension and transmission efficiency of a bush roller chain. Proceedings of the Institution of Mechanical Engineers, Part C: Journal of Mechanical Engineering Science **216**(4), 385–394. https://doi.org/10.1243/0954406021525179. URL http://journals.sagepub.com/doi/10.1243/0954406021525179

[10] N. Hollingworth (1987), A four-square chain wear rig. Tribology International **20**(1), 3–9. https://doi.org/10.1016/0301-679X(87)90002-8. URL https://linkinghub.elsevier.com/retrieve/pii/0301679X87900028

[11] R. Bolen, C.M. Archibald, in *ASEE Zone II Conference* (2017). URL http://zone2.asee.org/papers/proceedings/3/78.pdf

[12] M.O. Ross, K.M. Marshek (1982), Four-square sprocket test machine. Mechanism and Machine Theory **17**(5), 321–326. https://doi.org/10.1016/0094-114X(82)90014-3. URL https://linkinghub.elsevier.com/retrieve/pii/0094114X82900143

[13] S.C. Burgess, T. Pyper, C.S. Ling (2013), A linear actuated chain test rig capable of accelerated test speeds and continuous wear measurements. Proceedings of the Institution of Mechanical Engineers, Part C: Journal of Mechanical Engineering Science **227**(5), 1047–1055. https://doi.org/10.1177/0954406212451546. URL http://journals.sagepub.com/doi/10.1177/0954406212451546

[14] R. Aubert, X. Roizard, F. Grappe, F. Lallemand (2023), Tribological devices in cycling: A review. Proceedings of the Institution of Mechanical Engineers, Part P: Journal of Sports Engineering and Technology https://doi.org/10.1177/17543371231202562. URL http://journals.sagepub.com/doi/10.1177/17543371231202562

[15] R. Wragge-Morley, J. Yon, R. Lock, B. Alexander, S. Burgess (2018), A novel pendulum test for measuring roller chain efficiency. Measurement Science and Technology **29**(7), 075,008. https://doi.org/10.1088/1361-6501/aaa239. URL https://iopscience.iop.org/article/10.1088/1361-6501/aaa239

[16] T. Dowd, J. Miller, D. Heflin, W. Sweldens, A. Kraslinikau, J.A. Mansson, in *ISEA 2022 – The Engineering of Sport 14* (2022). https://doi.org/10.5703/1288284317530. URL https://docs.lib.purdue.edu/resec-isea/2022/session13/7/

[17] T. Dowd, J. Miller, D. Heflin, J.A. Mansson, W. Sweldens (2020). Bicycle trainer homologation apparatus. U.S. Provisional Patent Application. Filed

[18] D. Rome (2023). Chain cleaning: A complete guide from lazy to obsessive. URL https://velo.outsideonline.com/2018/05/chain-cleaning-and-maintenance-how-to/

[19] D. Rome (2020). How to wax a chain: an endless FAQ. URL https://velo.outsideonline.com/road/road-racing/

how-to-wax-a-chain-an-endless-faq/

[20] (2022). ANT+ Device Profile Fitness Equipment. URL www.thisisant.com

[21] A. Kerin. Chain Testing. URL https://zerofrictioncycling.com.au/chaintesting/

[22] J. Smith (2018). Friction Facts. URL https://web.archive.org/web/20180421123614/http://www.friction-facts.com/

[23] K.B. MacDougall, T.M. Falconer, B.R. MacIntosh (2022), Efficiency of cycling exercise: Quantification, mechanisms, and misunderstandings. Scandinavian Journal of Medicine and Science in Sports **32**(6), 951–970. https://doi.org/10.1111/sms.14149

[24] C. Abbiss, M. Quod, G. Levin, D. Martin, P. Laursen (2009), Accuracy of the Velotron Ergometer and SRM Power Meter. International Journal of Sports Medicine **30**(02), 107–112. https://doi.org/10.1055/s-0028-1103285. URL http://www.thieme-connect.de/DOI/DOI?10.1055/s-0028-1103285

[25] G. Ettema, H.W. Lorås (2009), Efficiency in cycling: A review. European Journal of Applied Physiology **106**(1), 1–14. https://doi.org/10.1007/s00421-009-1008-7